Sustained Subconjunctival Delivery of Infliximab Protects the Cornea and Retina Following Alkali Burn to the Eye

Chengxin Zhou,[1,2] Marie-Claude Robert,[3,4] Vassiliki Kapoulea,[1,2] Fengyang Lei,[1,2] Anna M. Stagner,[2,5] Frederick A. Jakobiec,[2,5] Claes H. Dohlman,[1,2] and Eleftherios I. Paschalis[1,2,6]

[1]Boston Keratoprosthesis Laboratory, Department of Ophthalmology, Massachusetts Eye and Ear and Schepens Eye Research Institute, Boston, Massachusetts, United States
[2]Harvard Medical School, Boston, Massachusetts, United States
[3]Department of Ophthalmology, Université de Montreal, Montreal, Quebec, Canada
[4]Centre Hospitalier de l'Université de Montreal, Hospital Notre-Dame, Montreal, Quebec, Canada
[5]David G. Cogan Ophthalmic Pathology Laboratory, Massachusetts Eye and Ear, Boston, Massachusetts, United States
[6]Disruptive Technology Laboratory (D.T.L.), Massachusetts Eye and Ear, Department of Ophthalmology, Harvard Medical School, Boston, Massachusetts, United States

Purpose. Tumor necrosis factor (TNF)-α is upregulated in eyes following corneal alkali injury and contributes to corneal and also retinal damage. Prompt TNF-α inhibition by systemic infliximab ameliorates retinal damage and improves corneal wound healing. However, systemic administration of TNF-α inhibitors carries risk of significant complications, whereas topical eye-drop delivery is hindered by poor ocular bioavailability and the need for patient adherence. This study investigates the efficacy of subconjunctival delivery of TNF-α antibodies using a polymer-based drug delivery system (DDS).

Methods. The drug delivery system was prepared using porous polydimethylsiloxane/ polyvinyl alcohol composite fabrication and loaded with 85 μg of infliximab. Six Dutch-belted pigmented rabbits received ocular alkali burn with NaOH. Immediately after the burn, subconjunctival implantation of anti-TNF-α DDS was performed in three rabbits while another three received sham DDS (without antibody). Rabbits were followed with photography for 3 months.

Results. After 3 months, the device was found to be well tolerated by the host and the eyes exhibited less corneal damage as compared to eyes implanted with a sham DDS without drug. The low dose treatment suppressed CD45 and TNF-α expression in the burned cornea and inhibited retinal ganglion cell apoptosis and optic nerve degeneration, as compared to the sham DDS treated eyes. Immunolocalization revealed drug penetration in the conjunctiva, cornea, iris, and choroid, with residual infliximab in the DDS 3 months after implantation.

Conclusions. This reduced-risk biologic DDS improves corneal wound healing and provides retinal neuroprotection, and may be applicable not only to alkali burns but also to other inflammatory surgical procedures such as penetrating keratoplasty and keratoprosthesis implantation.

Keywords: polydimethylsiloxane, tumor necrosis factor alpha, drug delivery system, antibody therapy, corneal wound healing, retinal protection, burn

Severe chemical burns of the cornea, even if promptly treated, often lead to blindness. Smoldering inflammation of the anterior segment results in corneal opacity, poor epithelial healing, sometimes ulceration and perforation, neovascularization and eventual scarring.[1] Rehabilitation is difficult because of extensive loss of limbal stem cells[2,3] and the fact that vessel ingrowth causes loss of immune privilege,[4] resulting in poor outcome of standard keratoplasty.[5,6] An artificial cornea, such as the Boston keratoprosthesis, is an alternative approach for these severe cases, but sterile melting of the cornea carrier graft tissue can occur in burned eyes and may affect keratoprosthesis retention.[7] It is also well known that ocular alkali burned patients have increased risk of glaucoma and subsequent irreversible vision loss.[8–10] Therefore, early suppression of inflammation and angiogenesis may improve the ocular healing processes and also help retain a keratoprosthesis.

The inflammation and neovascularization following a corneal chemical burn can be attributed to upregulation of angiogenic and proinflammatory factors. One of the most potent inflammatory cytokines is tumor necrosis factor (TNF)-α, which has been shown to cause corneal inflammatory injury.[11] In mice, TNF-α is highly upregulated within 24 hours after corneal alkali burn and later mediates neovascularization and scarring.[12] Prompt inhibition with an anti-TNF-α antibody (infliximab) after alkali burn has been shown to protect the cornea and promote healing.[12,13] This effect has also been demonstrated in animals with experimental keratoprosthesis[14] and in other settings.[15,16] Clinically, infliximab has been found to very effectively suppress inflammation after keratoprosthesis surgery in autoimmune diseases,[17,18] as well as in corneal ulceration.[19–21]

More recently, it has become clear that alkali burns can also adversely and irreversibly affect the retina and optic nerve. In

the most severe clinical cases, retinal scarring can later be observed if media are clear enough[22] or through a keratoprosthesis.[9] More often, the anatomical signs are subtler but just as functionally impairing. It has been shown in animals that alkali can cause substantial apoptosis of retinal ganglion cells, as well as optic nerve changes, which would be expected to result in glaucoma.[12] The effect of the alkali is not a direct one—the pH of the posterior eye segment remains normal and the alkali seems to be effectively buffered before reaching the retina (data submitted for publication).[12] Rather, the damage to the retina comes from cytokines, which can reach the retina within 24 hours. Tumor necrosis factor-α is quite likely a main offender and systemically administered TNF-α inhibitor (infliximab, a humanized chimeric monoclonal anti-TNFα antibody [Remicade, Jansen Biotech, NJ, USA]) can prevent retinal ganglion cell apoptosis to a considerable degree.[12] Thus, infliximab in clinically acceptable doses seems strongly neuroprotective and modes of delivery to the retina deserve attention.

There are limitations for biologic therapies related to their administration. Systemic administration of antibodies carries some risk of serious systemic adverse events.[23] Local administration with eye drops is limited by the large molecular size of infliximab (∼150 kD) and the corresponding slow diffusion, even in the absence of the epithelium.[13] Intravitreal injection of infliximab in humans has been associated with the development of severe uveitis in a large proportion of cases (37.5%).[24] Although intravitreal infliximab appears to benefit certain cases, these local safety concerns are a serious barrier to further pursue this method of drug administration.[25–28]

With the objective of overcoming some of these limitations, we recently developed a drug delivery system (DDS) for local administration of anti-TNF-α antibody to the eye.[29] The drug delivery system is made of a porous polydimethylsiloxane (PDMS) scaffold loaded with a polyvinyl alcohol (PVA) hydrogel containing the drug. We have performed drug stability, release, and in vivo safety evaluations of the DDS loaded with infliximab. The drug has remained stable after sterilization with γ radiation and exposure to room temperature for 1 year. After an initial burst, sustained zero-order release of anti-TNF-α antibody was achieved for 1 month in vitro. Here, the device was implanted subconjunctivally in rabbits with ocular alkali burns and the effect of infliximab elution on the cornea and retina was evaluated for 3 months.

MATERIALS AND METHODS

Rabbit Alkali Burn Model

All rabbits were treated in accordance with the Association for Research in Vision and Ophthalmology Statement on the Use of Animals in Ophthalmic and Vision Research, and the experimental protocol was approved by the Animal Care Committee of the Massachusetts Eye and Ear Infirmary. All experiments were carried out on the OD eyes under a surgical microscope and general anesthesia. Six Dutch-Belted female rabbits (Covance, Dedham, MA, USA) weighing between 2 and 2.5 kg were used. Rabbits were anesthetized by intramuscular injection of ketamine hydrochloride INJ, USP (35 mg/kg; KetaVed, VEDCO, St. Joseph, MO, USA) and xylazine (5 mg/kg; AnaSed, LLOYD, Shenandoah, IA. USA). Topical anesthetic (0.5% proparacaine hydrochloride, Bausch & Lomb, Tampa, FL, USA) was applied to the operative eyes. Alkali burn was performed in the anesthetized rabbits using an 8-mm diameter cotton sponge soaked in 2 N NaOH and applied to the center of a cornea for 10 seconds, followed by immediate eye irrigation with saline solution for 20 minutes. Buprenorphine

(0.03 mg/kg; Buprenex Injectable, Reckitt Benckiser Healthcare Ltd, United Kingdom) was administered subcutaneously prior to the burn procedure for long-term pain management. After the surgery, yohimbine (0.1 mg/kg; Yobine, LLOYD) was administered in a marginal ear vein to reverse the effect of xylazine, and a transdermal fentanyl patch (12 μg/hour; LTS Lohmann Therapy System, Corp., NJ, USA) was placed on the right ear to alleviate pain for 3 postoperative days.

Implantation of DDS

Antitumor necrosis factor-α DDS was prepared as previously described.[29] Lyophilized infliximab powder was dissolved in 10% (wt/v) PVA and then infused into a porous PDMS carrier using vacuum for 2 hours. Infliximab-loaded PDMS was then air-dried and stored at room temperature in a sterile vial. Each DDS implant was precut to approximately 4 mm in length and 1 mm in diameter, yielding a weight of 13 mg and containing approximately 85 μg of infliximab. Drug-loaded DDS implants ($n = 3$) and sham DDS implants as controls (DDS without drug loaded, $n = 3$) were implanted in six rabbits immediately after the corneal alkali burn. Subconjunctival implantation of the DDS was performed in the inferior bulbar conjunctiva to avoid unexpected dislocation of the polymer. Briefly, a narrow lateral subconjunctival pocket with a length of 4 mm was made cautiously with fine spring surgical scissors. The subconjunctival pocket was positioned laterally and 1 mm away from the lower fornix. The precut DDS strip implant was then inserted into the subconjunctival pocket. Both ends of the DDS implant were then sutured to the scleral wall using an 8-0 vicryl suture. Erythromycin ophthalmic ointment (0.5%, Bausch & Lomb) was given topically to the operative eyes twice a day for 1 week after surgery.

Clinical Evaluation

Clinical evaluation was performed on all rabbits before the chemical burn and DDS implantation surgery and postoperative days 0, 1, 2, 5, and every 7 days for 3 months thereafter. For these evaluations, the rabbits were anesthetized by intramuscular injection of ketamine hydrochloride (20 mg/kg) and xylazine (5 mg/kg) and topical anesthetic 0.5% proparacaine hydrochloride was applied to the operative eyes. All treated and control eyes were photographed using a digital SLR camera (Nikon, Tokyo, Japan) attached to a surgical microscope (S21; Carl Zeiss, Jena, Germany) at standard magnifications. Photographs were analyzed using ImageJ 1.50e software (http://imagej.nih.gov/ij/; provided in the public domain by the National Institutes of Health [NIH], Bethesda, MD, USA). The resolution of each image was 4288 × 2848 pixels. Corneal epithelial defects were stained with fluorescein and imaged using a portable slit-lamp (Keeler 3010-P-2001, PA) equipped with cobalt blue filter and a mounted digital camera at 10× magnification. Ocular lubricant (GenTeal, Alcon, Fort Worth, TX, USA) was applied as needed during these procedures. Reversal of anesthesia was obtained through yohimbine (0.1 mg/kg) IV administration in a marginal ear vein.

Quantification of corneal neovascularization (CNV) area and epithelial defect area was performed using ImageJ software (NIH). The areas of corneal vasculature and fluorescein stain were outlined with the polygon selection tool and calculated using the ImageJ software (NIH). Each area measurement ($pixel^2$) was normalized by the relative whole cornea area ($pixel^2$) in the same image to eliminate the small variation in camera magnification, yielding the CNV or epithelial defect area / whole cornea ratio (%).

Subjective assessments of CNV, central corneal, and peripheral corneal opacity were performed by three indepen-

dent scientists (MR, FL, VK) using photographs in a single masked fashion to minimize observation bias. To differentiate corneal opacification due to immediate alkali reactions (e.g., saponification) seen in the central cornea, from secondary inflammatory cell-mediated remodeling manifested in the peripheral cornea, the central and peripheral corneas were scored separately for opacity. Central and peripheral corneal opacity was scored in 0.5 increments on a scale of 0 to 4, where 0 = completely clear; 1 = slightly hazy, iris/pupil easily visible; 2 = slightly opaque, iris/pupil still detectable; 3 = opaque, iris/pupil hardly detectable; and 4 = completely opaque with no view of the iris/pupil.

Corneal neovascularization was scored based on the intensity of the vessels in the cornea (Int.V), where 0 = no visible vessel, 1 = faint thin vessels, 2 = mild thickened vessels, 3 = moderate thickened vessels, and 4 = thick vessels. The length of vessel (Lth.V) invading into the cornea was scored using the following grade system: 0 = no corneal vessel, 1 = from limbus to far periphery, 2 = from limbus to mid periphery, and 3 = from limbus to central cornea. The clock hours (CHs; 30 degrees = 1 CH) involved in the CNV region were also estimated. Again, the images were scored in 0.5-unit increments. An overall CNV score was derived from the above three assessments (overall CNV score = Int.V + Lth.V + CHs/3). Because the range in CHs was 0 to 12 hours, the number was divided by 3 to provide normalization to the scale 0 to 4, in order to match the scale of Int.V and Lth.V. Agreement between the three raters was statistically assessed using the intraclass correlation coefficient (ICC) test.

Histologic and Immunohistochemical Examinations

At the end of the follow-up, rabbits were euthanized using Fatal Plus intravenously (Sodium pentobarbital; 100 mg/kg, Vortech, Dearborn, MI, USA). Both eyes and the lower lid with the conjunctival tissue holding the DDS implant were harvested and fixed in 4% paraformaldehyde (PFA) overnight at 4°C. The tissues were then embedded in optical coherence tomography (OCT) and flash-frozen. Tissue section slides of whole globes and DDS-harboring eyelids were prepared with a cryostat (CM1950, Leica Biosystems, Buffalo Grove, IL, USA) at 10 μm thickness and transferred to positively charged glass slides (Superfrost glass slides, Thermo Fisher, IL, USA). Hematoxylin/eosin staining was performed for general histologic observation. For immunohistochemistry, tissue sections were permeabilized with 0.2% Triton-X100 for 5 minutes and incubated with 1% bovine serum albumin (BSA) for 1 hour at room temperature. Primary antibodies were diluted in 1% BSA and incubated with the tissue samples overnight at 4°C. Secondary antibodies were incubated with the samples for 2 hours at room temperature. Infiltration of immune cells in tissues was evaluated with mouse anti-CD45 monoclonal antibody (1:100, SC-70690, Santa Cruz, Dallas, TX, USA). Tumor necrosis factor-α expression was immunolocalized by a mouse anti-TNF-α monoclonal antibody conjugated with FITC (1:100, NBP1-51502, Novus, Littleton, CO, USA). Retinal nerve fiber layer (RNFL) and cells at the ganglion cell layer (GCL) were analyzed using anti-β3 tubulin monoclonal antibody (1:100, MA1118, Thermo Scientific, Rockford, IL, USA). The contralateral, nonburned eye of each rabbit was used as an internal control. Residual infliximab antibody in the DDS and surrounding tissues was detected with Alexa Fluor 546 conjugated goat anti-human IgG secondary antibody (1:300, A-21089, Thermo Scientific).

Mounting media with 4′,6-diamidino-2-phenylindole (DAPI) (UltraCruz, Santa Cruz) was used together with glass cover slips for imaging using the Zeiss Axio Imager M2 (Carl Zeiss)

fluorescence microscope with 20× dry and 63× oil immersion objective lenses. The total number of cells expressing TNF-α or CD45 in a whole cornea section was counted using the "Analyze Particles" tool in NIH ImageJ software. The mean values obtained from three tissue section samples are reported.

Optic nerve cross sections were examined for glaucomatous damage by using a modified paraphenylenediamine (PPD) staining protocol to stain the myelin sheath of all axons, and the axoplasma of damaged axons, as previously described.[14] Sections from burned and contralateral nonburned eyes were used for comparison. A portion of the nerve between the orbit and chiasm was surgically dissected, and fixed with half strength Karnovsky's fixative (2% formaldehyde + 2.5% glutaraldehyde, in 0.1 M sodium cacodylate buffer, pH 7.4 [Electron Microscopy Sciences, Hatfield, PA, USA]) for a minimum of 24 hours at 40°C. After fixation, samples were rinsed with 0.1 M sodium cacodylate buffer, postfixed with 2% osmium tetroxide in 0.1 M sodium cacodylate buffer, then dehydrated with graded ethyl alcohol solutions, transitioned with propylene oxide and resin infiltrated in tEPON-812 epoxy resin (Tousimis, Rockville, MD, USA) utilizing an automated EMS Lynx 2 EM tissue processor (Electron Microscopy Sciences). Processed tissues were oriented in tEPON-812 epoxy resin and polymerized in silicone molds using an oven set for 60°C for 48 hours. Semithin cross-sections were cut at 1-μm with a Histo diamond knife (Diatome, Hatfield, PA, USA) on a Leica UC-7 ultramicrotome (Leica Microsystems, Buffalo Grove, IL, USA) and collected on slides, then dried on a slide warmer. The slides were stained with filtered 2% aqueous PPD (MP Biomedicals LLC, Solon, OH, USA) solution for 1 hour at room temperature, rinsed in tap and deionized water solutions, air-dried, then mounting media and a glass coverslip was applied over the sections for light microscopic analysis.

Cross-sections of different anatomic levels were taken and imaged with 100× objective in a light microscope. More than 40 pictures of each cross-section were taken. The fields were spaced in a regular fashion across the entire nerve section, taking care to avoid field overlap. A rectangular box was then drawn near the center of each image to eliminate the shaded or out-of-focus areas. The cropped pictures were systematically analyzed to quantify axon numbers per unit area, axon area, and circularity with "Particle Analyze" tool in ImageJ (NIH). Circularity was defined as $4\pi[Area]/[Perimeter]^2$ with a value of 1.0 indicating a perfect circle. As the value approaches 0.0, it indicates an increasingly elongated shape. Axons with circularity <0.2 were excluded from the counting.

The retinal nerve fiber layer and number of cells in the retinal GCL of rabbits were analyzed in histologic sections using β3-tubulin monoclonal antibody (1:100, MA1118, Thermo Scientific) and DAPI. β3-tubulin+ DAPI+ cells in GCL were manually counted and normalized to the total measured retinal length. A minimum of three different nonconsecutive tissue sections per eye was analyzed and three rabbits per sample. To assess GCL cell loss in the burned eyes, the contralateral nonburned eye of each rabbit was used as internal control (reference of normal cell count). Data were presented in percentages of the remaining cells, with 100% representing the number of cells in the contralateral nonburned eye (β3-tubulin+ cell density in burned eye/β3-tubulin+ cell density in contralateral eye*100).

Statistics

Quantitative results were reported as means ± standard deviations. The normality of data was assessed by Shapiro-Wilk test. Depending on the normality, Student's t-test or Mann-Whitney U test was performed to compare the means between the anti-TNF-α DDS group and the sham DDS group. One-way

and 2-way ANOVA were performed in datasets containing multiple variables, followed with Holm-Sidak pairwise multiple comparison correction test. Analyses were performed using R Studio (Boston, MA, USA). Interrater agreement was assessed with the ICC test for absolute agreement. Intraclass correlation coefficient scores between 0.8 and 0.9 assumed "good agreement" and between 0.9 and 0.99 "excellent agreement." Intraclass correlation coefficient measurements were provided with 95% confidence interval. Mixed ANOVA was performed in datasets containing dependent variables (e.g., CNV, opacity scores, and corneal defect area) with fixed variables being time and treatment. Analyses were performed using the Statistical Package of Social Sciences (SPSS, IBM, NY, USA). Linear and second order polynomial functions were generated in Graph-Pad Prism Version 6.0 (GraphPad, La Jolla, CA, USA) to fit data points.

RESULTS

Safety of the DDS and Infliximab Stability

A predominantly granulomatous local response to the polymer implants with (Fig. 1A) and without (Fig. 1C) infliximab was seen following DDS placement in the subepithelial tissues of the conjunctival fornix. A spectrum of granulomatous inflammation was seen in both groups. The majority of the inflammatory cells were mononucleated epithelioid cells (Fig. 1B) in the lumen engulfing remnants of the implant with occasional giant cells (Figs. 1B, 1D). There was minimal to no inflammation noted in the adjacent pseudocapsule and connective tissues. While one rabbit exhibited occasional aggregates of mucus near the DDS implantation site, the subconjunctival DDS implantation appeared to be safe at the ocular surface with no overt sign of toxicity. The small incision in the conjunctival tissue created for inserting the DDS strip healed within 7 days (Fig. 1G). A photograph of the DDS demonstrated its shape and porous texture of the DDS (Fig. 1H).

Antitumor necrosis factor-α DDS showed positive immunoreactivity with a secondary antibody against human IgG 3 months after implantation (Fig. 1E), whereas none of sham DDS showed immunoreactivity to IgG (Fig. 1F). Infliximab antibodies were not completely depleted from the DDS by the end of 3 months. Eyes implanted with anti-TNF-α DDS also showed immunoreactivity to anti-human IgG secondary antibody (Supplementary Fig. S1). Positive human IgG signal was found around and within small vessels in the cornea, conjunctiva, iris, and choroid 3 months after implantation of the DDS. Conversely, eyes implanted with sham DDS had no infliximab signal in any of the aforementioned tissue. The conjunctival tissue harboring the anti-TNF-α DDS also showed marked levels of human IgG in a diffusion gradient pattern (Supplementary Fig. S1). Infliximab presence in ocular tissue 3 months after DDS implantation suggests slow and continuous diffusion of antibody from the DDS.

Effect of Anti-TNFα DDS Treatment in Corneal Neovascularization After Corneal Alkali Burn

Although all rabbits developed CNV after alkali burn (Figs. 2A–F), the anti-TNF-α DDS group exhibited lower mean percentage of CNV area and overall CNV score compared to the sham DDS group. The relative CNV area in the anti-TNF-α DDS group 92 days after burn was $13 \pm 5\%$, whereas in the sham DDS group was $31 \pm 14\%$. However, no statistically significant difference was present between the two groups (P
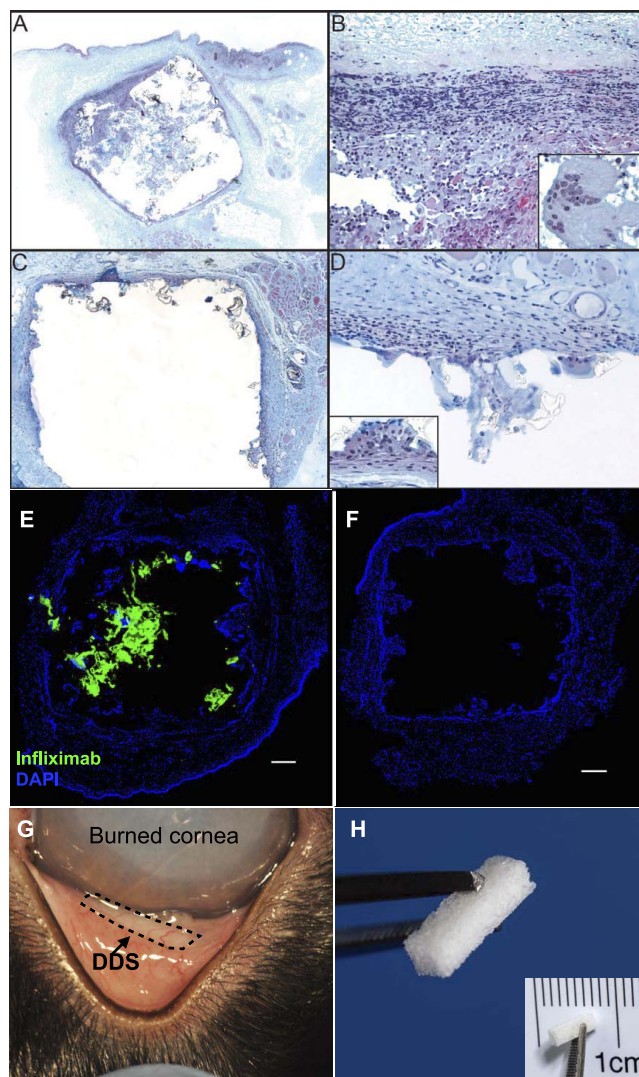
FIGURE 1. In vivo cellular response to subconjunctival DDS implants and infliximab stability. (A) An implant containing infliximab has elicited an inflammatory response in the lumen. Note that the surrounding fibrous pseudocapsule is not inflamed. (B) Most of the inflammation is granulomatous and composed of mononucleated epithelioid cells and occasional giant cells (_inset_). (C) An implant without drug manifests a milder granulomatous response in the lumen with no inflammation in the surrounding connective tissues. (D) Epithelioid cells and giant cells line the luminal inner wall occupied by a drug-free implant (sham DDS). The _inset_ demonstrates an adherent nodule of granulomatous inflammation. (A–D) Masson trichrome staining, A: ×50, B: ×200 (_inset_ ×400), C: ×50, D: ×200 (_inset_ ×400). (E–F) Immunofluorescence staining against human IgG of the subconjunctival tissue harboring the DDS. (E) Note the intense signal of human IgG in the infliximab-loaded DDS 3 months after rabbit subconjunctival implantation. (F) The sham DDS showed no immunoreactivity with the antibody. Images taken at ×20 magnification with tiling. _Scale bar_: 250 μm. (G) Light photograph of the anti-TNF-α DDS at 15 days after implantation subconjunctivally in the lower lid of a burned rabbit. (H) A photograph of the DDS showing the porous architecture. The antibody is loaded into the 3D porous network using PVA carrier at desired concentrations. _Insert_ shows the size and shape of the DDS. The drug delivery system can be trimmed and shaped as required.

$= 0.228$) likely due to the considerable variability in the sham DDS group (Fig. 2G).

The corneal neovascularization score in the anti-TNF-α DDS group at 92 days was 6.4 ± 2.6, whereas in the sham DDS
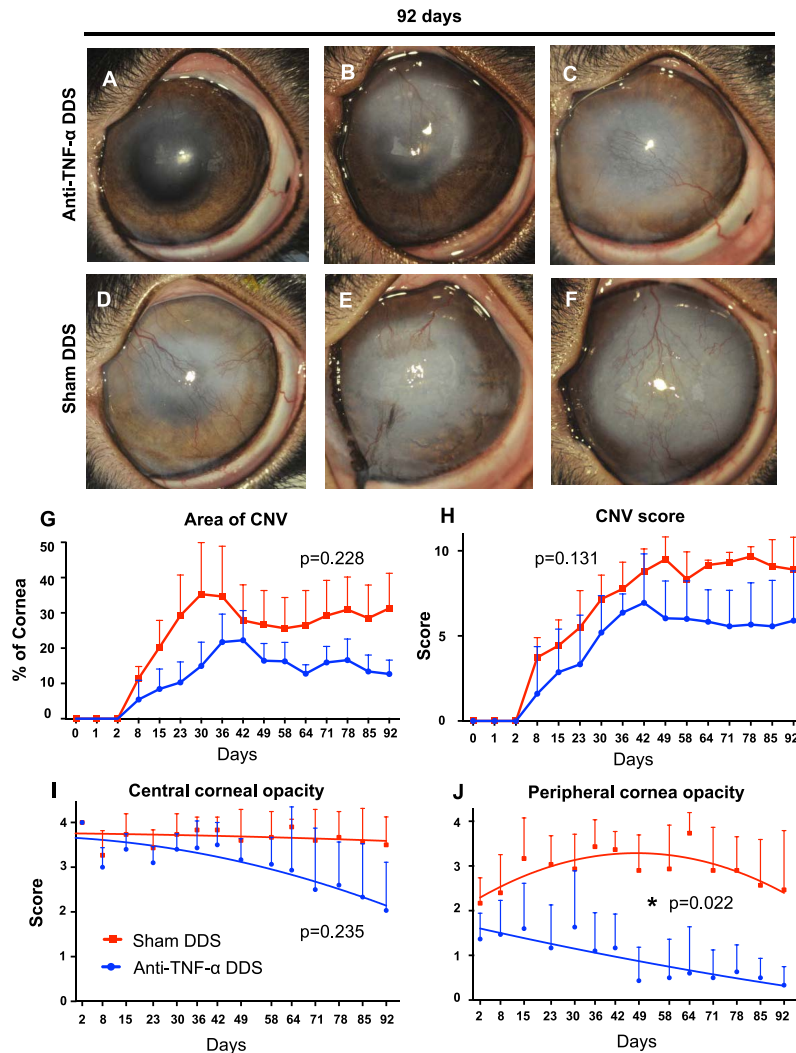
FIGURE 2. Effect of anti-TNF-α DDS in reducing CNV and opacification after alkali burn. Photographs of the rabbit eyes treated with anti-TNF-α DDS (**A–C**) and with sham DDS (**D–F**) 3 months after corneal alkali burn. (**G, H**) Although not statistically significant, anti-TNF-α DDS treated rabbits had smaller areas of CNV compared to sham DDS treated ($P = 0.228$; mixed ANOVA). Similar progression patterns were found from the single-masked assessment of CNV ($P = 0.131$; mixed ANOVA). (**I, J**) Independent, single-masked assessment of central and peripheral corneal opacity showed that anti-TNF-α DDS treated rabbits had similar central corneal opacity as the sham DDS group, but accelerated peripheral corneal clearance compared to sham DDS treated, which exhibited persistent corneal opacity ($P < 0.05$; mixed ANOVA). Opacity score ranges from 0 to 4 (0 = clear, 4 = opaque).

group was 8.4 ± 0.7 but no statistically significant difference (Fig. 2H, $P = 0.131$). The scores from all masked raters were in agreements ($ICC_{central}$ corneal opacity: 0.886, $P < 0.0001$ [0.835–0.923, confidence interval (CI): 95%], $ICC_{peripheral}$ corneal opacity: 0.889, $P < 0.0001$ [0.838–0.925, CI: 95%]). One rabbit in the sham DDS group (Fig. 2E) developed severe central corneal necrosis that significantly and artificially reduced the mean central CNV area in this group.

Effect of Anti-TNFα DDS Treatment in Corneal Opacity After Corneal Alkali Burn

All rabbits treated with anti-TNF-α DDS exhibited continuous decrease in the central and peripheral corneal opacity, during the 3-months evaluation period, as compared to the sham DDS group (Figs. 2I, 2J). Both groups had similar central corneal opacity within the studied time period ($P = 0.235$; mixed ANOVA; Fig. 2I), but the anti-TNF-α DDS group had significantly lowered peripheral corneal opacity than the sham DDS group ($P < 0.05$; mixed ANOVA; Fig. 2J). The scores from the

three masked raters were in agreement (ICC_{CNV}: 0.892, $P < 0.0001$, CI: 95%: 0.762–0.943).

Effect of Anti-TNF-α DDS Treatment on Corneal Epithelial Wound Healing After Corneal Alkali Burn

Rabbits treated with anti-TNF-α DDS had significantly reduced area of epithelial defect as compared to sham DDS treated within the studied time frame (Fig. 3G, $P = 0.04$, mixed ANOVA), except for a short period of time (36–42 days) where both groups had similar defect area. Rabbits treated with the anti-TNF-α DDS exhibited faster re-epithelialization of the cornea and complete corneal epithelial wound closure 64 ± 8 days after the burn. Conversely, all sham DDS treated eyes exhibited incomplete epithelial wound closure by the end of the study. In fact, at 92 days, the corneal epithelial defect area in the sham DDS group accounted for $6.3 \pm 4.7\%$ of the total cornea ($n = 3$) versus no defect area in the anti-TNF-α DDS group ($n = 3$, $P < 0.05$, Figs. 3C, CF). Two linear regressions
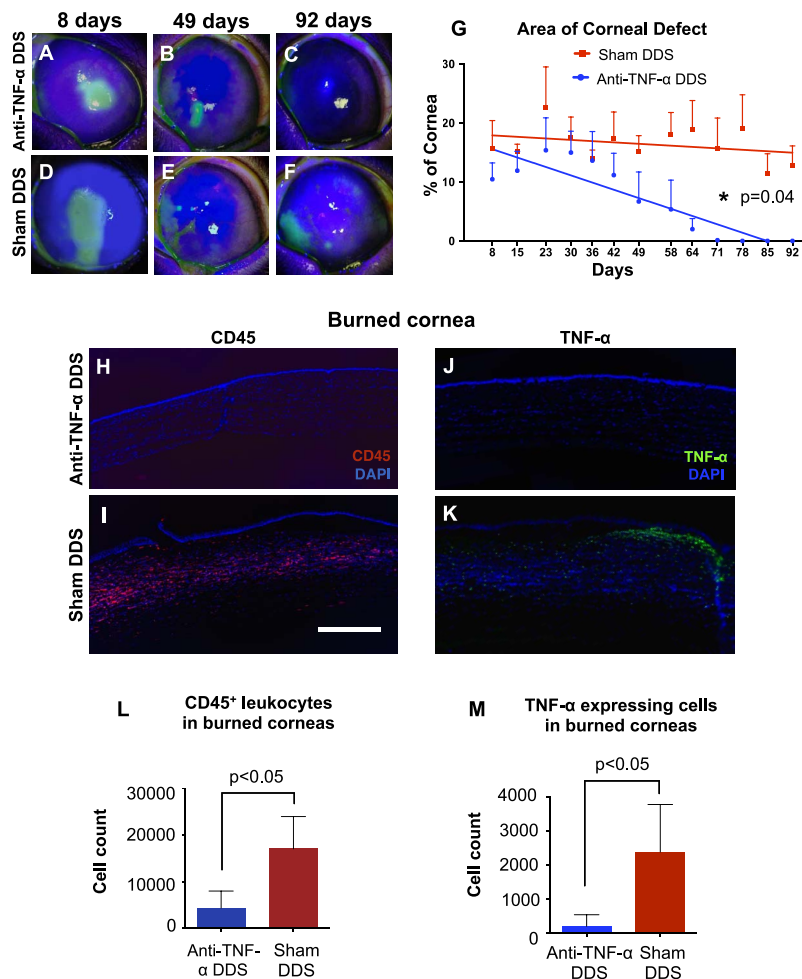
FIGURE 3. Effect of anti-TNF-α DDS in corneal epithelial defect closure and inflammation after alkali burn. Representative slit-lamp biomicroscopic images of the injured corneal with fluorescein staining 8 days (**A**, **D**), 49 days (**B**, **E**), and 92 days (**C**, **F**) after corneal alkali burn. (**A–F**) ×10 (**G**) anti-TNF-α DDS treatment significantly promoted corneal re-epithelization as compared to sham DDS treatment ($P < 0.05$; mixed ANOVA). All corneas treated with anti-TNF-α DDS achieved complete corneal re-epithelialization within 71 days. Conversely, none of the sham DDS treated eyes achieved complete re-epithelialization and wound closure during the 92 days of follow-up. Immunolocalization using anti-CD45 antibody in tissue sections showed that anti-TNF-α DDS treated rabbits (**H**) exhibited significantly reduced CD45 expression in the cornea as compared to sham DDS treated eyes (**I**) at 3 months. Immunolocalization using anti-TNF-α antibody in tissue sections showed that anti-TNF-α DDS treatment (**J**) significantly suppressed TNF-α expression in the corneal as compared to sham DDS treated eyes (**K**), **H–K** ×20 with tiling. *Scale bar*: 500 μm. (**L**) Numbers of CD45$^+$ leukocytes/cornea section in the burned eyes. $n = 3$ rabbits/group. (**M**) Numbers of TNF-α expressing cells/cornea section in the burned eyes. $n = 3$ rabbits/group.

were fitted to the two datasets. The slope of the best-fitted line for anti-TNF-α DDS group was −0.2023, $R^2 = 0.47$ and the slope of sham DDS group was −0.0349, $R^2 = 0.0190$.

Effect of Anti-TNFα DDS Treatment in TNF-α Expression and Leukocyte Infiltration

Immunohistochemistry of rabbit cornea sections showed that anti-TNF-α DDS suppressed CD45$^+$ cell infiltration and TNF-α expression in the burned corneas as compared to the sham DDS group. Antitumor necrosis factor-α DDS treated rabbits had significantly less CD45$^+$ cells in the cornea (Fig. 3H) at 3 months as compared to the sham DDS group that had abundant CD45$^+$ leukocytes in the central and midperipheral corneal stroma (Fig. 3I). CD45$^+$ cell quantification showed a reduced population of leukocytes (mean = 4322 cells/cornea) in the anti-TNF-α treated group as compared to the sham DDS treated group (mean = 17,049 cells/cornea, $P < 0.05$; Fig. 3L). Further, a significant number of CD45$^+$ cells were observed in

the limbal epithelium, iris, angle area, and corneal endothelium of the sham DDS corneas while the eyes treated anti-TNF-α DDS presented few CD45$^+$ cells in these tissues.

Consistent with the results of CD45$^+$ leukocyte infiltration in the cornea, anti-TNF-α DDS treated eyes exhibited remarkably less TNF-α expression (Fig. 3J) as compared to the sham DDS treated eyes (Figs. 3K, 3M, $P < 0.05$). Tumor necrosis factor-α expression was predominant in ulcerated corneal area (e.g., the central anterior corneal stroma; Fig. 3K) and in the vicinity of the corneal neoangiogenesis.

Ocular Pathology

Preservation of the corneal endothelial mosaic and anterior segment structure was seen in all of the eyes treated with anti-TNF-α DDS (Fig. 4A). In eyes with sham DDS implants, all anterior segments were abnormal to varying degrees. These eyes demonstrated epithelial ulceration with bullae formation, subjacent collagen denaturation, chronic anterior stromal
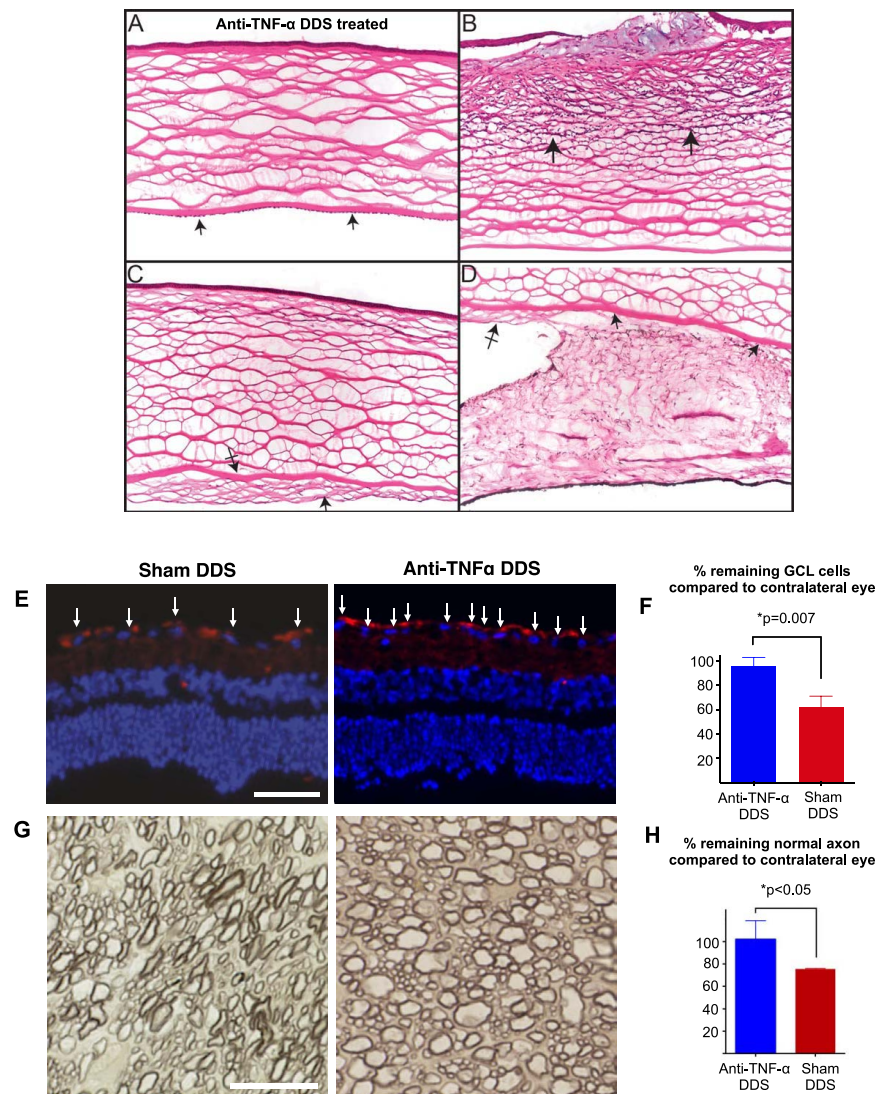
FIGURE 4. Ocular pathology and retinal/optic nerve neuropathy. (A–D) Appearance of the anterior ocular structures. (A) Treated cornea displays intact, noninflamed layers including preserved endothelium (arrows). (B) Nontreated (sham) cornea with disruption and absence of the central epithelium, separation of surrounding epithelium by bullae and loss of endothelial cells. There are inflammatory cells between the anterior corneal stromal lamellae (arrows). (C) A retrocorneal fibrous membrane (arrow) is adjacent to Descemet's membrane (crossed arrow) in this untreated cornea. (D) Peripheral anterior synechiae (arrows) in an untreated eye merges with the retrocorneal fibrous membrane (crossed arrow), A–D, ×100. (E–H) Retinal and optic nerve degeneration 3 months after ocular alkali burn. (E) Representative ×20 immunohistofluorescence retinal images (β3-tubulin = red and DAPI = blue) of burned eyes treated either with sham or anti-TNF-α DDS. Sham treated eyes exhibited significantly higher loss of cells in the GCL as compared to anti-TNF-α DDS treated eyes. Antitumor necrosis factor-α DDS treated eyes exhibited increased β3-tubulin expression in the GCL as compared to sham DDS treated. Scale bar: 50 μm. (G) Representative microscopy images of p-phenylenediamine stained optic nerve sections of burned rabbit eyes. Consistent with the immunohistofluorescence results, sham DDS treated eyes exhibited significantly increased optic nerve axon degeneration and reduced optic nerve axon density as compared to anti-TNF-α DDS treated eyes. Antitumor necrosis factor-α treatment retain the normal fascicle packing and regular myelin wraps of the optic nerve axons. Scale bar: 10 μm. (F) Quantification of β3-tubulin+ cells in GCL. GCL cells of sham DDS treated eyes had significantly lower density compared to anti-TNF-α DDS treated eyes, $n = 3$, $P < 0.05$. (H) Sham DDS treated eyes exhibited significantly increased loss of optic nerve axons as compared to anti-TNF-α DDS treated eyes, $n = 3$, $P < 0.05$. All measurements were normalized according to the contralateral nonburned and nontreated eye.

keratitis, and endothelial cell attenuation (Fig. 4B). Retrocorneal fibrous membrane formation (Fig. 4C) and peripheral anterior synechiae (Fig. 4D) were other anterior segment findings observed in the sham DDS treated eyes but not in the anti-TNF-α DDS treated eyes. Ocular phthisis and disorganization of intraocular structures was developed in one eye treated with sham DDS. No evidence of inflammation was detected in the posterior segment (retina, vitreous, and choroid) of eyes from both groups.

Retinal and Optic Nerve Degeneration

This study demonstrated marked retinal and optic nerve degeneration following corneal alkali burn. Retinal neurodegeneration was inhibited using the anti-TNF-α DDS treatment, but not by the sham DDS. Antitumor necrosis factor-α treated eyes exhibited a 4.3% mean reduction of retinal GCL cell count as compared to the corresponding contralateral nonburned eye. Conversely, sham DDS treated eyes exhibited a

significant 38.1% mean reduction in GCL cell count ($P < 0.05$, Student's *t*-test; Figs. 4E, 4F). Likewise, burned eyes treated with anti-TNF-α DDS showed no reduction in optic nerve axon density as compared to the optic nerves from the corresponding contralateral nonburned eye. However, sham DDS treated eyes exhibited a significant 24.5% loss in optic nerve axons, as compared to the contralateral nonburned eye. Burned eyes treated with anti-TNF-α DDS had significantly higher optic nerve density as compared to burned sham DDS treated eyes ($P < 0.05$, unpaired Student's *t*-test; Figs. 4G, 4H).

DISCUSSION

Our results confirm that TNF-α is a major mediator of inflammation in the cornea and, perhaps even more importantly, in the retina following ocular alkali burn. The upregulation of TNF-α expression in burned corneas was positively correlated with large corneal infiltration of leukocytes, delayed corneal wound healing, endothelial cell loss, ulceration, corneal opacity, and neovascularization, as well as with retinal ganglion cell loss and optic nerve degeneration. Conversely, prompt treatment with anti-TNF-α antibody (infliximab) significantly suppressed complications of the burned eye. The infliximab-loaded DDS delivered the drug with considerable therapeutic effect, not only to the cornea but also to the retina.

It can be questioned whether the retinal and optic nerve alterations have been mediated by intraocular pressure elevation due to anterior peripheral synechiae. Peripheral corneal inflammation, which was markedly increased in the sham DDS treated eyes, may have contributed to angle closure and subsequent intraocular pressure elevation. Alternatively, and perhaps more likely, severe anterior segment inflammation in the early stages after the burn may have had a direct inflammatory effect on the posterior structures. Of importance here is that etanercept (another antibody of TNF-α) has been shown to prevent retinal ganglion cell loss in a rat model of hypertensive glaucoma.[30]

This study also demonstrated that the DDS implant is clinically well tolerated in the subconjunctival space of the lower eyelid fornix of the rabbits. Still, by histology, there was some granulomatous inflammation detected in the spaces occupied by all the implants—the most conspicuous example was noted in an eye with anti-TNF-α loaded DDS. This would suggest antigenicity engendered by the chimeric antibody. There was, however, no significant lymphocytic or granulomatous response in the enveloping pseudocapsule or in the connective tissues beyond the implant, indicating the limited focal response to the DDS. The rabbits did not display any systemic illness, consistent with the mouse study. The hosts' conjunctival area healed with no visible defect on the surface 7 days after implantation. A possible concern of subconjunctival implantation of the anti-TNF-α DDS could be device extrusion, as we observed in one rabbit. However, this complication was related to loose sutures, which can be avoided.

The drug delivery system is composed of a porous hydrophobic and nondegradable PDMS polymer, which has been studied extensively for biocompatibility in vivo and in vitro in microfluidic devices,[31] and tissue engineering.[32] The inflammatory responses observed in DDS implantation can be attributed of natural body reaction to foreign material, which is an indispensable processed during implant integration and healing processes. The reactions presented in our study have also been described in the literature where PDMS was evaluated in different mouse, rat, rabbit models as the reference material to other test materials.[33] A study by Petillo

et al.[34] demonstrated similar percentage of Ia⁺ macrophages in the exudate of PDMS and empty control implants. In short, it is generally accepted that PDMS induces mild host tissue response, but it is safe for long-term implantation.[31-35]

The effect of the DDS drug delivery to the retina is of particular importance. Burned eyes treated with anti-TNF-α DDS exhibited only minimal retina ganglion cell loss compared to those receiving the sham DDS, which exhibited a significant ~40% reduction. Likewise, anti-TNF-α DDS treated eyes showed no reduction in optic nerve axon density, whereas sham DDS treated eyes exhibited a significant ~30% reduction. These findings may be clinically important. If a TNF-α inhibitor can be administered to the retina in sufficient doses by any safe and efficient route soon after an alkali burn—ideally in the emergency room immediately following the lavage—it is likely that some damage to the eye can be prevented. Since corneal transparency can now be restored with a keratoprosthesis in even severe alkali burns, it can be argued that protection of the retina and the optic nerve should be given primary attention. Since damage to these structures is irreversible, dosage and route of administration of infliximab should be chosen with priority to retinal neuroprotection.

Thus the efficacy, safety, and practicality of the various modes of delivery to the eye must be compared: systemic infusion, subcutaneous injection, local drops, gels or DDS, subconjunctival or subtenon injection or DDS, or intravitreal injection. Toxicity and pharmacokinetic studies are clearly warranted. Previous studies with infliximab drops in mouse and rabbit models focused on the early biological responses following injury, where the studied time frame was within 10 days. The infliximab was shown to penetrate into the anterior stroma of the injured corneas only in the absence of the epithelium.[13] However, efficacy is expected to be reduced following re-epithelialization or conjunctivalization of the cornea in the later healing stage. It has not been demonstrated whether infliximab in drop form can protect the retina. Subconjunctival administration of infliximab, on the other hand, appears to bypass the barrier of the epithelium quite effectively and it has already been shown that a single subconjunctival injection of infliximab results in drug infiltration into the cornea and other anterior chamber tissues but, again, any effect on the retina was not described.[13]

It remains to be determined whether subconjunctival implantation of an infliximab-loaded DDS is therapeutically superior to a single subconjunctival injection. Except for the strong initial burst release of infliximab, the DDS has been shown to have a nearly zero-order release kinetics over 1 month in vitro.[29] In this study, eyes with anti-TNF-α DDS showed presence of infliximab antibody around and within small vessels in the cornea, conjunctiva, iris, and choroid 3 months after implantation of the DDS (Supplementary Fig. S1). This suggests that the anti-TNF-α antibody is continuously released by the DDS for at least 3 months and the antibody finds its way to various ocular tissues. The therapeutic effect of sustained anti-TNF-α delivery was also observed in one rabbit with early DDS extrusion (42 days) due to loose conjunctival sutures. This rabbit exhibited increased infiltration of leukocytes in the cornea and increased loss of RGCs as compared to the rabbits that retained the anti-TNF-α DDS for 3 months (Supplementary Fig. S2). Even though this finding is based on only one rabbit, it may suggest that the effect of prolonged release of anti-TNF-α antibody to the eye may be therapeutically important and warrants further investigation. Although more complex in insertion and removal, the bioavailability and sustainability of infliximab delivery to both the anterior and posterior segments of the eye are possibly enhanced compared to a single subconjunctival injection. The effect achieved in our rabbit model with a very small dose of infliximab (85 μg in the

current DDS) compared to that of standard systemic route (2–10 mg/kg) is striking. This means that the systemic effect of the subconjunctival DDS-delivered dose should be trivial in a human compared to that of the standard intravenous dose. It can be speculated that the DDS can be modified to fit into the lower lid fornix (cul-de-sac) to give therapeutic effect at least to the cornea. This modality does not require implantation, the dose is adjustable, and most importantly reversible by removing the DDS.

These results confirm that TNF-α is a major mediator of inflammation in the eye following ocular surface burn with alkali and that TNF-α inhibition may protect the eye from extensive damage to the cornea, retina, and optic nerve, and may even improve the prognosis of a subsequent corneal transplant. The finding that a low dose of local infliximab delivered via the subconjunctival space can result in substantial retinal neuroprotection should have applications beyond alkali burns. For example, in keratoprosthesis surgery where systemic delivery of infliximab has been shown to be protective, or in surgical procedures of the eye that induce ocular inflammation, infliximab prophylaxis may be beneficial. The ability of the DDS to deliver various biologic agents to the retina, such as anti-VEGF or combination anti-TNF-α/anti-VEGF agents is an intriguing concept that requires future attention.

References

1. Pfister RR, Pfister DA. Alkali injuries of the eye. In: Krachmer JH, Mannis MJ, Holland EJ, eds. *Cornea*. St. Louis, MO: Mosby; 1997.

2. Kenyon KR, Tseng SC. Limbal autograft transplantation for ocular surface disorders. *OPHTHA*. 1989;96:709–722; discussion 722–723.

3. Fagerholm P, Lisha G. Corneal stem cell grafting after chemical injury. *Acta Ophthalmol Scand*. 1999;77:165–169.

4. Dohlman TH, Omoto M, Hua J, et al. VEGF-trap aflibercept significantly improves long-term graft survival in high-risk corneal transplantation. *Transplantation*. 2015;99:678–686.

5. Abel R, Binder PS, Polack FM, Kaufman HE. The results of penetrating keratoplasty after chemical burns. *Trans Am Acad Ophthalmol Otolaryngol*. 1975;79:584–595.

6. Williams KA, Esterman AJ, Bartlett C, Holland H, Hornsby NB, Coster DJ. How effective is penetrating corneal transplantation? Factors influencing long-term outcome in multivariate analysis. *Transplantation*. 2006;81:896–901.

7. Dohlman CH, Cruzat A, White M. Die Boston-Keratoprothese 2014 – Ein Schritt in der Entwicklung künstlicher Hornhäute. *Spektrum Augenheilkd*. 2015;28:226–233.

8. Tsai JH, Derby E, Holland EJ, Khatana AK. Incidence and prevalence of glaucoma in severe ocular surface disease. *Cornea*. 2006;25:530–532.

9. Cade F, Grosskreutz CL, Tauber A, Dohlman CH. Glaucoma in eyes with severe chemical burn, before and after keratoprosthesis. *Cornea*. 2011;30:1322–1327.

10. Lin MP, Ekşioğlu Ü, Mudumbai RC, Slabaugh MA, Chen PP. Glaucoma in patients with ocular chemical burns. *Am J Ophthalmol*. 2012;154:481–485.e481.

11. Dekaris I, Zhu SN, Dana MR. TNF-alpha regulates corneal Langerhans cell migration. *J Immunol*. 1999;162:4235–4239.

12. Cade F, Paschalis EI, Regatieri CV, Vavvas DG, Dana R, Dohlman CH. Alkali burn to the eye: protection using TNF-α inhibition. *Cornea*. 2014;33:382–389.

13. Ferrari G, Bignami F, Giacomini C, Franchini S, Rama P. Safety and efficacy of topical infliximab in a mouse model of ocular surface scarring. *Invest Ophthalmol Vis Sci*. 2013;54:1680–1688.

14. Crnej A, Omoto M, Dohlman TH, et al. Effect of penetrating keratoplasty and keratoprosthesis implantation on the posterior segment of the eye. *Invest Ophthalmol Vis Sci*. 2016;57:1643–1648.

15. Li Z, Choi W, Oh H-J, Yoon K-C. Effectiveness of topical infliximab in a mouse model of experimental dry eye. *Cornea*. 2012;31(suppl 1):S25–S31.

16. Kim JW, Chung SK. The effect of topical infliximab on corneal neovascularization in rabbits. *Cornea*. 2013;32:185–190.

17. Dohlman CH, Dudenhoefer EJ, Khan BF, Dohlman JG. Corneal blindness from end-stage Sjögren's syndrome and graft-versus-host disease. *Adv Exp Med Biol*. 2002;506:1335–1338.

18. Robert M-C, Crnej A, Shen LQ, et al. Infliximab after Boston keratoprosthesis in Stevens–Johnson syndrome: an update. *Ocul Immunol Inflamm*. 2016;1–5.

19. Thomas JW, Pflugfelder SC. Therapy of progressive rheumatoid arthritis-associated corneal ulceration with infliximab. *Cornea*. 2005;24:742–744.

20. Odorcic S, Keystone EC, Ma JJK. Infliximab for the treatment of refractory progressive sterile peripheral ulcerative keratitis associated with late corneal perforation: 3-year follow-up. *Cornea*. 2009;28:89–92.

21. Pham M, Chow CC, Badawi D, Tu EY. Use of infliximab in the treatment of peripheral ulcerative keratitis in Crohn disease. *Am J Ophthalmol*. 2011;152:183–188.e182.

22. Smith RE, Conway B. Alkali retinopathy. *Arch Ophthalmol*. 1976;94:81–84.

23. Codreanu C, Damjanov N. Safety of biologics in rheumatoid arthritis: data from randomized controlled trials and registries. *Biologics*. 2015;9:1–6.

24. Wu L, Arevalo JF, Hernandez-Bogantes E, Regatieri CV, Roca JA, Farah ME. Intravitreal tumor necrosis factor-alpha inhibitors for neovascular age-related macular degeneration suboptimally responsive to antivascular endothelial growth factor agents: a pilot study from the Pan American Collaborative Retina Study Group. *J Ocul Pharmacol Ther*. 2013;29:366–371.

25. Rodrigues EB, Farah ME, Maia M, et al. Therapeutic monoclonal antibodies in ophthalmology. *Prog Retin Eye Res*. 2009;28:117–144.

26. Theodossiadis PG, Liarakos VS, Sfikakis PP, Vergados IA, Theodossiadis GP. Intravitreal administration of the anti-tumor necrosis factor agent infliximab for neovascular age-related macular degeneration. *Am J Ophthalmol*. 2009;147:825–830.

27. Wu L, Hernandez-Bogantes E, Roca JA, Arevalo JF, Barraza K, Lasave AF. Intravitreal tumor necrosis factor inhibitors in the treatment of refractory diabetic macular edema: a pilot study from the Pan-American Collaborative Retina Study Group. *Retina*. 2011;31:298–303.

28. Pascual-Camps I, Hernández-Martínez P, Monje-Fernández L, et al. Update on intravitreal anti-tumor necrosis factor alpha

therapies for ocular disorders. *J Ophthalmic Inflamm Infection*. 2014;4:26–26.

29. Robert M-C, Frenette M, Zhou C, et al. A drug delivery system for administration of anti-TNF-α antibody. *Trans Vis Sci Tech*. 2016;5(2):11.

30. Roh M, Zhang Y, Murakami Y, et al. Etanercept, a widely used inhibitor of tumor necrosis factor-α (TNF-α), prevents retinal ganglion cell loss in a rat model of glaucoma. *PLoS One*. 2012; 7:e40065.

31. Ren X, Bachman M, Sims C, Li GP, Allbritton N. Electroosmotic properties of microfluidic channels composed of poly(dimethylsiloxane). *J Chromatograph*. 2001:117–125.

32. King KR, Terai H, Wang CC, Vacanti JP, Borenstein JT. Microfluidics for tissue engineering microvasculature: endo-thelial cell culture. In: *Micro Total Analysis Systems*. Netherlands: Springer; 2001:247–249.

33. Belanger MC, Marois Y. Hemocompatibility, biocompatibility, inflammatory and in vivo studies of primary reference materials low-density polyethylene and polydimethylsiloxane: a review. *J Biomed Mater Res*. 2001;58:467–477.

34. Petillo O, Peluso G, Ambrosio L, Nicolais L, Kao WJ, Anderson JM. In vivo induction of macrophage Ia antigen (MHC class II) expression by biomedical polymers in the cage implant system. *J Biomed Mater Res A*. 1994;28:635–646.

35. Kim SH, Moon J-H, Kim JH, Jeong SM, Lee S-H. Flexible, stretchable and implantable PDMS encapsulated cable for implantable medical device. *Biomed Eng Lett*. 2011;1:199–203.